Electrical conductivity studies of nanocrystalline Dy^{3+} doped $CaMoO_4$ synthesized by sol-gel process

Paramananda Jena[1], N. Nallamuthu[1], M. Venkateswarlu[2], N. Satyanarayana[1*]

[1] Department of Physics, Pondicherry University, Pondicherry- 605 014, India.
[2] R & D, Amara Raja Batteries Ltd, Tirupati - 517 520 A.P, India.

Abstract

Oxygen ion conducting solid electrolytes have many device applications such as sensors, solid oxide fuel cells, oxygen pumps, electrochemical reactors and steam electrolysis cells. Among these, solid oxide fuel cells (SOFCs) have attracted great attention in electrochemical devices because of their high energy conversion efficiency, little pollution and widely flexible fuel choices. Scheelite type based oxide ion conducting materials like $PbWO_4$, $BaMoO_4$, $SrMoO_4$ having high ion conductivity compared to others and these can be used as electrolyte for intermediate temperature solid oxide fuel cell (ITSOFC) applications. The present work aims to develop nanocrystalline Dy^{3+} doped $CaMoO_4$ to increase the ionic conductivity for ITSOFC applications. Nanocrystalline dysprosium doped $CaMoO_4$ samples were prepared by using acrylamide assisted gel combustion process. All the samples were characterized by TG/DTA, XRD, FTIR and SEM techniques. For the sintered dysprosium doped $CaMoO_4$ crystalline samples, electrical conductivity were evaluated from the analysis of the impedance plots, obtained at different temperatures.

Key words: Acrylamide assisted gel combustion Process, Scheelite type nanocrystalline oxide, XRD, FTIR, SEM, Impedance and Electrical conductivity.

1. Introduction

Generally, Oxygen ion conductors are much imperative samples and can be used in various technological devices such as solid oxide fuel cells, oxygen sensors, electrochemical oxygen pumps, etc. [1-2]. Several families of oxygen ion conductors are being investigated for intermediate temperature solid oxide fuel cells (ITSOFCs) like fluorite type (stabilized ZrO_2, CeO_2 and δ-Bi_2O_3) oxides, pervoksite type ($LaGaO_3$, $BaCeO_3$ and $SrCeO_3$) oxides, brownmillerite type ($Ba_2In_2O_3$) oxides, aurivillius type (BIMEVOX) oxides, pyrochlore type ($Gd_2Zr_2O_7$) oxides and scheelite type ($PbWO_4$) oxides [3-5].

Scheelite type oxides exhibit high ion conductivity, which are comparable with the yttria stabilized zirconia.[6-8] Takao Esaka et al., have investigated the composition dependent of electrical conductivity for $PbWO_4$ scheelite type samples and reported the electrical conductivity, 4.2×10^{-2} Scm^{-1} at 800 ^oC for $Pb_{0.8}La_{0.2}WO_{4.1}$. [7] V.Thangadurai et al. preapared ABO_4 (A= Ca, Sr, Ba; B= Mo,W) scheelite type samples and they noticed that the scheelite type samples ($PbWO_4$, $SrWO_4$) show the higher electrical conductivity between the temperatures 500 ^oC to 900 ^oC [8]. The nanocrystalline metal oxide compounds have the small grain size, which lead to the further increase of ionic conductivity and also the stabilization of high temperature crystal structure. In recent years, nanostructured ceramics have been investigated due to the presence of a large fraction of grain boundaries that can lead to remarkable or enhanced electrical, magnetic, mechanical, optical, sensing and biomedical properties compared with the microstructured samples [9]. Dy_2O_3 is one of the rare earth oxides and it has high mechanical and thermal stability, suitable for glass, optic and ceramic applications [10]. Hence, in the present study, nanocrystalline Scheelite type dysprosium doped $CaMoO_4$ compounds were prepared by using acrylamide assisted gel combustion process and also all the compounds were characterized by TG/DTA, XRD, FTIR and SEM techniques. Also, for sintered nanocrystalline dysprosium doped $CaMoO_4$ pellets, electrical conductivity was evaluated from the measured impedance data at different temperatures.

2. Experimental

2.1. Acrylamide assisted gel combustion process

Different compositions of nanocrystalline Dy^{3+} doped $CaMoO_4$ samples were synthesized by acrylamide assisted gel combustion process using acrylamide and citric acid as fuels. The precursor chemicals (Calcium nitrate, dysprosium nitrate and ammonium molybdate) were taken according to their respective molecular weight percentage. Calcium nitrate is dissolved in distilled water and mixed with citric acid and acrylamide as solution. Dysprosium nitrate solution is prepared by dissolving the required amount of dysprosium nitrate in the distilled water. Ammonium molybdate is added with distilled water and stirred the solution till the transparent solution is

 CTSI-Cleantech 2013, www.ct-si.org, ISBN 978-1-4822-0594-7

formed. Dysprosium nitrate solution is mixed with the previous Calcium nitrate solution under constant stirring. Half an hour later, ammonium molybdate solution is also added to the previous mixture solution and stirred continuously till the formation of the gel at 80 ^{o}C. The prepared gels were dried and heated at various temperatures to form the nanocrystalline dysprosium doped $CaMoO_4$ samples and are characterized by TG-DTA, FTIR, XRD and SEM techniques.

2.2. Measurement Techniques

The TG-DTA curves of the dysprosium doped $CaMoO_4$ samples were recorded using TA instruments SDT Q600 V20.5 DTA-TGA thermal analyzer. The fine powdered dried gel sample of ~6 mg was placed in the alumina crucible heated at the rate of 10 ^{o}C per minute from 40 ^{o}C to 900 ^{o}C under nitrogen atmosphere. The fine powdered mixture of calcined gel sample and KBr powder in 1:20 ratio are pelletized using KBr press to form the thin transparent pellet samples, prepared at different calcined temperatures. FTIR spectra were recorded using Schimadzu FTIR/8300/8700 spectrophotometer in the frequency range of 4000 – 400 cm^{-1} with 2 cm^{-1} resolution for 20 scans. XRD patterns were recorded for the fine powdered dried gels using panalytical X'pert pro diffractometer with Cu $K_{\alpha,}$ as the source radiation of wavelength (λ=1.5418 A^{o}), from 10^{0} to 80 ^{0}. The synthesized nanocrystalline dysprosium doped $CaMoO_4$ powder samples were pressed into 10mm diameter and 2-3 mm thickness pellets at 5000 kg/cm^2 using KBr press. The prepared pellets were sintered at various temperatures to perform the electrical characterization of the nanocrystalline dysprosium doped $CaMoO_4$ samples.

Results and discuss

TG-DTA

Fig. 1. shows the TG-DTA curves of nanocrystalline dysprosium doped $CaMoO_4$ gel samples. The observed wide endothermic peak between 100 ^{o}C and ~150 ^{o}C and the simultaneously observed weight losses for the dried gel samples are due to the evaporation of water molecules existing in the sample.The observed exothermic DTA curves at 200 ^{o}C and 250 ^{o}C respectively are due to the decomposition of citric acid and nitrates from calcium nitrate as well as from dysprosium nitrate. The observed exothermic DTA curves is intensified with the increase of dysprosium content in the $CaMoO_4$ sample. This may be due to the different binding energies of calcium nitrate and dysprosium nitrate. Doping of dysprosium in the $CaMoO_4$, increases the total quantity of nitrates in the precursor, which increases the oxidant ratio and helpful for combustion reaction. However, after 600 ^{o}C, there is no weight loss is observed in the TG curve, which indicates that there is complete decomposition of organic derivatives from the sample and the same is also confirmed from FTIR and XRD results.

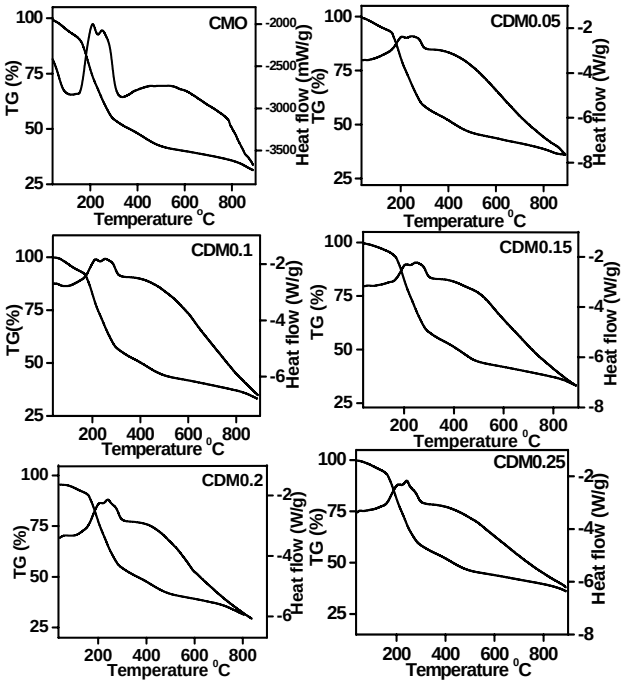

Fig.1. TG-DTA curves of the various compositions of dysprosium doped $CaMoO_4$ gel samples dried at 60 ^{o}C.

FTIR

Fig.2. shows the FTIR spectra of all the compositions of dysprosium doped $CaMoO_4$ dried gel samples calcined at 900 ^{o}C. From the fig.2, the appearance of the IR peak at ~820 cm^{-1} is attributed to the Mo-O stretching vibration

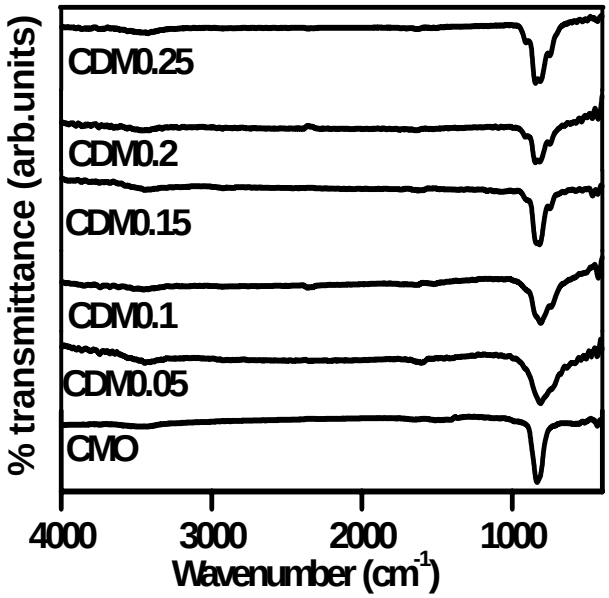

Fig.2. FTIR spectra of all the compositions of dysprosium doped $CaMoO_4$ dried gel samples calcined at 900 ^{o}C.

and also the observed IR band at 746 cm^{-1} is assigned to the Dy-O network formation. When the dopant quantity increases, the defects concentrations increase and hence, at the higher doping compositions, the newly observed IR bonds 660 and 450 cm^{-1} are respectively attributed to the formation of Dy-O-Mo and Dy-O-Ca bonds. Further, the formation of phase and microstructure are conformed from XRD and SEM results.

XRD

Fig. 3. shows the XRD patterns of the dysprosium doped $CaMoO_4$ samples, obtained at 900 ^oC. The observed crystalline peaks in the XRD patterns are confirmed the formation of the Scheelite type $CaMoO_4$ crystalline phase, by comparing the obtained XRD peaks with the standard ICDD 01-085- 1267 data. The crystallite size of the all the compositions of dysprosium doped $CaMoO_4$ samples were calculated using Scherrer's formula: $D = 0.9\lambda/ (\beta \cos \theta)$, where λ is the X-ray wave length (0.15418 nm), β is full width half.

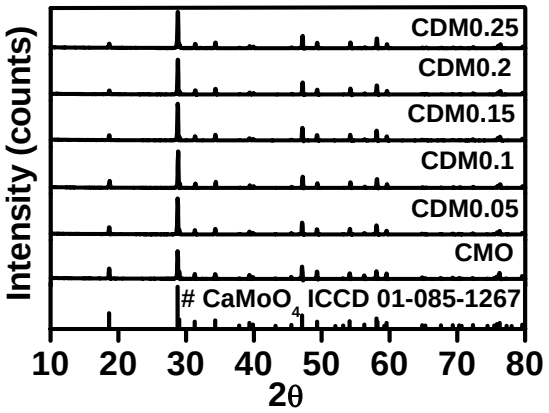

Fig.3. XRD patterns of the various compositions of dysprosium doped $CaMoO_4$ samples obtained at 900 ^0C.

SEM measurement

Fig.4. shows SEM image of the particular composition of dysprosium doped $CaMoO_4$ ($Ca_{0.95}Dy_{0.05}MoO_{4.025}$) powder, obtained at 900 ^oC. SEM micrograph showed agglomerated spherical particles of $Ca_{0.95}Dy_{0.05}MoO_{4.025}$ powder sample. Their particle sizes are measured and found to be less than 100 nm.

Electrical conductivity studies

At ambient temperature, electrical impedance data are measured for all the compositions of dysprosium doped $CaMoO_4$ pellet samples sintered at 900 ^oC. The total resistance obtained from the intercept of the depressed semicircle with the real axis and the total conductivity is calculated using the resistance and the pellet dimensions. In the Dy doped Calcium molybdate samples, the $Ca_{0.95}Dy_{0.05}MoO_{4.025}$ composition showed higher conductivity and the conductivity versus Dy doped Calcium molybdate compositions is shown in figure 5.

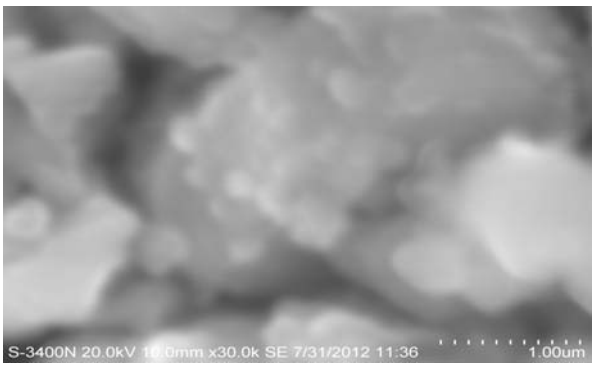

Fig.4. SEM image of dysprosium doped $CaMoO_4$ ($Ca_{0.95}Dy_{0.05}MoO_{4.025}$) powder obtained at 900 ^oC.

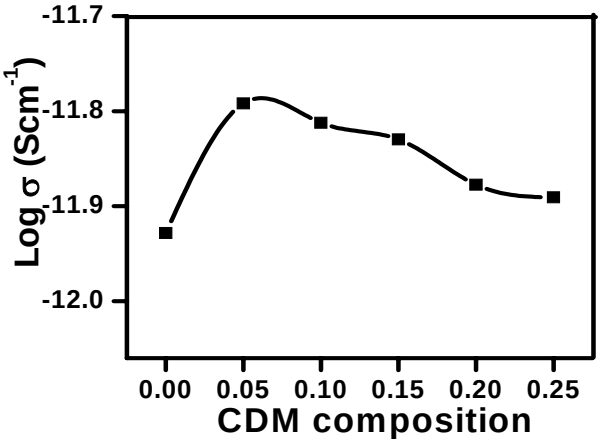

Fig.5. Total conductivity of all the compositions of Dy doped $CaMoO_4$ samples obtained at ambient temperature.

Fig.6. shows the impedance plots obtained at various temperatures for the nanocrystalline $Ca_{0.95}Dy_{0.05}MoO_{4.025}$ sample. From fig. 6, the two depressed semicircles are observed in the impedance plots, where, large semicircle in the lower frequency region indicates the grain boundary response and the lower semicircle in the higher frequency region indicates the grain interior response of the nanocrystalline $Ca_{0.95}Dy_{0.05}MoO_{4.025}$ sample.

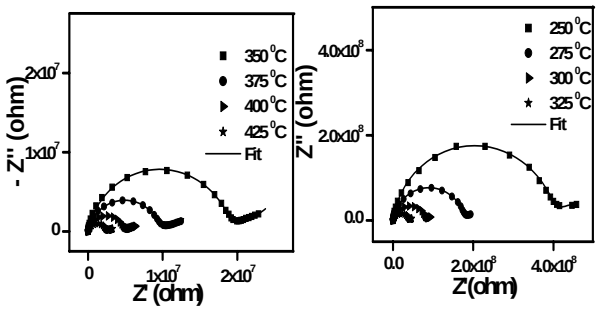

Fig.6.Impedance plots (Z' vs – Z") for $Ca_{0.95}Dy_{0.05}MoO_{4.025}$, obtained at various temperatures.

CTSI-Cleantech 2013, www.ct-si.org, ISBN 978-1-4822-0594-7

The total conductivity (σ) [i.e., grain interior conductivity (σ_{gi}) and grain boundary conductivity (σ_{gb})] for nanocrystalline $Ca_{0.95}Dy_{0.05}MoO_{4.025}$ sample is calculated using the formula.

$$\sigma = (t/A) \times (1/R)$$

Where R is the resistance of the sintered pellet, t is the thickness of the sintered pellet and A is the area of the sintered pellet. Fig.7. shows the log σT vs 1000/T plots for the total conductivity of $Ca_{0.95}Dy_{0.05}MoO_{4.025}$ sample pellet. sintered at 900 ^{o}C.

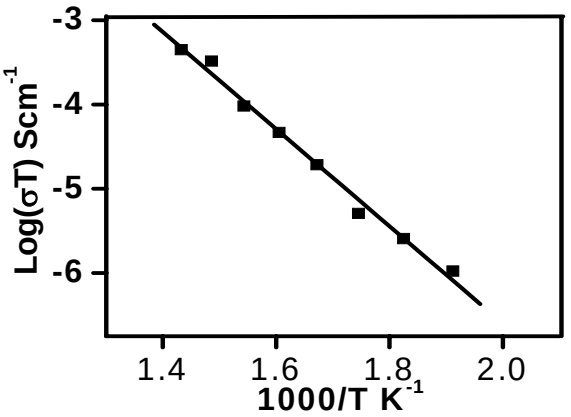

Fig.7. Log σT vs 1000/T plots for total conductivity of $Ca_{0.95}Dy_{0.05}MoO_{4.025}$ sintered at 900 ^{o}C.

The activation energy is calculated from the Log σT vs. 1000/T plots of nanocrystalline $Ca_{0.95}Dy_{0.05}MoO_{4.025}$ sample and it is found to be 1.145±0.046 eV for the total conductivity. The observed higher conductivity and activation energy may be due to the formation and also the migration of oxygen ion charge carriers in the nanocrystalline dysprosium doped $CaMoO_4$ sample ($Ca_{0.95}Dy_{0.05}MoO_{4.025}$).

Conclusion:

Different compositions of the nanocrystalline dysprosium doped $CaMoO_4$ samples were synthesized by using acrylamide assisted gel combustion process. TG/DTA curves of the dysprosium doped $CaMoO_4$ samples showed the complete crystallization at ~600 ^{o}C. XRD patterns confirmed the phase of the Scheelite type $CaMoO_4$ nanocrystalline samples and the crystallite size calculated by using the Scherer's formula, is found to be <100nm. Formation of MoO_3 is identified by FTIR spectra. SEM micrograph showed an agglomerated spherical particles and their particle sizes are found to be <100 nm. The $Ca_{0.95}Dy_{0.05}MoO_{4.025}$ sample showed the highest conductivity at ambient temperature compared to all other compositions of Dy doped $CaMoO_4$ samples. The total conductivity of dysprosium doped $CaMoO_4$ ($Ca_{0.95}Dy_{0.05}MoO_{4.025}$) sample obtained at 425 ^{o}C is found to be 6.46 x 10^{-7} Scm^{-1}. Also, the $Ca_{0.95}Dy_{0.05}MoO_{4.025}$ sample exhibits higher activation energy. The observed higher conductivity and activation energy may be due to the formation and also the migration of oxygen ion charge carriers in the nanocrystalline Dy doped $CaMoO_4$ sample ($Ca_{0.95}Dy_{0.05}MoO_{4.025}$).

Acknowledgement:

Dr N.S is gratefully acknowledged DST, AICTE, CSIR, and DRDO Govt. of India, for receiving the financial support in the form of major research projects. Authors also acknowledge CIF, Pondicherry University for using TG/DTA and SEM facilities.
* Corresponding author: N. Satyanarayana
Phone: +91413 2654404
E-mail: nallanis2011@gmail.com

References

[1] J.P.P. Huijsmans, Curr. Opin. Solid State Mater. Sci., 5, 317, (2001) .
[2] P.N. Dyer, R.E. Richards, S.L. Russek, D.M. Taylor, Solid State Ionics, 134, 21, (2000).
[3] John B. Goodenough, Annu. Rev. Mater. Res.,. 33, 91,2003.
[4] V.V. Khartona, F.M.B. Marquesa, A. Atkinson, Solid State Ionics, 174, 135, (2004).
[5] G.G. Zhang, Q F Fang1, X.P. Wang and Z.G. Yi, J. Phys.: Condens. Matter, 15, 4135, (2003).
[6] N. Nallamuthu, I. Prakash, N. Satyanarayana, M. Venkateswarlu, Materials Research Bulletin 46, 32, (2011).
[7] T.Esaka, Solid State Ionics 136-137, 1, (2000).
[8] V. Thangadurai, S.Knilllmayer,W.Weppner, Material science and engineering B, 106, 228, (2004).
[9] Martin G. Bellino, Diego G. Lamas and Noemi E.Walsoe de Reca, Adv. Funct. Mater., 16, 107, (2006).
[10] Tung-Ming Pan, and Chao-Wen Lin, J. Phys. Chem. C 114, 17914–17919 (2010).